Supporting Information

Inhibition of high-fat diet-induced obesity via reduction of ER-resident protein Nogo occurs through multiple mechanisms

Xiaolin Wang[1], Yanfang Yang[1], Dan Zhao[1], Shuang Zhang[2], Yi Chen[1], Yuanli Chen[2], Ke Feng[1], Xiaoju Li[1], Jihong Han[1,2], Yasuko Iwakiri[3], Yajun Duan[2*], Xiaoxiao Yang[2*]

Content

Table S1. Impact of Nogo deficiency on serum lipid, aminotransferase and glucose levels

	Normal chow		High-fat diet	
	Control	**Nogo KO**	**Control**	**Nogo KO**
T-CHO (mmol/l)	3.05 ± 0.07	2.76 ± 0.04	6.11 ± 0.20	6.10 ± 0.10
HDL (mmol/l)	1.84 ± 0.03	1.79 ± 0.04	2.50 ± 0.03	2.58 ± 0.03
LDL (mmol/l)	0.14 ± 0.01	0.15 ± 0.004	0.47 ± 0.02	0.53 ± 0.01
TG (mmol/l)	1.35 ± 0.05	0.99 ± 0.03***	1.3 ± 0.05	1.0 ± 0.04$^{\#\#}$
FFA (μmol/l)	429 ± 22	328 ± 23*	519 ± 27	479 ± 23
ALT (U/l)	19.7 ± 1.3	19.7 ± 1.5	37.7 ± 6.0	37.1 ± 3.9
AST (U/l)	133 ± 6.7	123 ± 5.3	140 ± 8.7	141 ± 5.7
ALP (U/l)	80.9 ± 3.5	81.1 ± 3.5	91.1 ± 7.1	68.9 ± 3.2$^{\#}$
Glucose (mmol/l)	10.1 ± 0.57	8.0 ± 0.27*	19.7 ± 0.8	15.1 ± 0.23$^{\#\#\#}$

Male Nogo KO and littermate control mice (~6-week old) were fed normal chow or high-fat diet for 14 weeks. At the end of experiment, serum samples were collected and used to determine levels of T-CHO, HDL, LDL, TG, FFA and glucose, and activities of ALT, AST and ALP. *p < 0.05, ***p < 0.001 *versus* control mice fed normal chow; $^{\#}p$ < 0.05, $^{\#\#}p$ < 0.01, $^{\#\#\#}p$ < 0.001 *versus* control mice fed high-fat diet (n=8). ALP, alkaline phosphatase; ALT, aspartate transaminase; AST, alanine aminotransferase; FFA, free fatty acid; HDL, high-density lipoprotein cholesterol; LDL, low-density lipoprotein cholesterol; Nogo, reticulon-4; T-CHO, total cholesterol; TG, triglyceride.

Table S2. Injection of Nogo siRNA has no effect on serum cholesterol and aminotransferase levels

	High-fat diet	
	Control	**Nogo KD**
T-CHO (mmol/l)	7.23 ± 0.10	7.40 ± 0.13
HDL (mmol/l)	2.22 ± 0.09	2.44 ± 0.11
LDL (mmol/l)	1.05 ± 0.02	1.12 ± 0.06
ALT (U/l)	221 ± 21	204 ± 27
AST (U/l)	245 ± 11	257 ± 20
ALP (U/l)	71.5 ± 1.1	70.9 ± 1.6

Male C57BL/6J mice (~6-week old, 5/group) were fed high-fat diet for 25 weeks, then randomly divided into two groups and received tail vein injection of scrambled siRNA (Control) or Nogo siRNA (Nogo KD) (40 μg per mouse) once every three days for 5 times. Mice were sacrificed three days after the last injection. Serum samples were collected and used to determine levels of T-CHO, HDL and LDL, and activities of ALT, AST and ALP (n=5). ALP, alkaline phosphatase; ALT, aspartate transaminase; AST, alanine aminotransferase; HDL, high-density lipoprotein cholesterol; KD, knockdown; LDL, low-density lipoprotein cholesterol; Nogo, reticulon-4; T-CHO, total cholesterol.

Table S3. Sequences of siRNA for *in vivo* study

	sense	antisense
Ctrl siRNA	UUCUCCGAACGUGUCACGUTT	ACGUGACACGUUCGGAGAATT
si-Nogo-1	GGAUCUCAUUGUAGUCAUATT	UAUGACUACAAUGAGAUCCTT
si-Nogo-2	GCAGUGUUGAUGUGGGUAUUUTT	AAAUACCCACAUCAACACUGCTT
si-Nogo-3	CACAUAAACUAGGAAGAGATT	UCUCUUCCUAGUUUAUGUGTT

Table S4. Sequences of primers for qRT-PCR

Genes	Primers	Sequence (5'-3')	Product (bp)
mAcaca	forward	GAAGTCAGAGCCACGGCACA	119
	reverse	GGCAATCTCAGTTCAAGCCAGTC	
mAco2	forward	GCACAAAATGGCGCCTTACA	188
	reverse	GGTTCAACCGTTTACGGACAA	
mAcox1	forward	GAAGATGAGGGAATTTGGCA	128
	reverse	CCTGATTCAGCAAGGTAGGG	
mAcox2	forward	GACATGGCAAGAACAGCCTT	125
	reverse	TGTCCGTCATAACAGCCAAG	
mAdiponectin	forward	GAGAGAAAGGAGATGCAGGTCT	198
	reverse	AGCGAATGGGTACATTGGGA	
mAdipoR1	forward	GTAAACATTTCCGGCCCCTC	304
	reverse	TGTGATGGTGGACACTTAGGC	
mArg-1	forward	GGTGGATGCTCACACTGACAT	121
	reverse	GAATCCTGGTACATCTGGGAAC	
mAtf4	forward	CCTGAACAGCGAAGTGTTGG	134
	reverse	TGGAGAACCCATGAGGTTTCA	
mAtgl	forward	GAGCCCCGGGGTGGAACAAGAT	231
	reverse	AAAAGGTGGTGGGCAGGAGTAAGG	
mBip	forward	CGTGTGTGTGAGACCAGAAC	224
	reverse	TAGGTGGTCCCCAAGTCGAT	
mChop	forward	CCACCACACCTGAAAGCAGAA	150
	reverse	GGTGCCCCCAATTTCATCT	
mCidea	forward	CATGATCTTGGAAAAGGGACAG	156
	reverse	ATCGTGGCTTTGACATTGAGAC	
mCol6α1	forward	GCGATTGCCTTCCAAGACTG	311
	reverse	CAGTCGGTGTAGGTGCCTTT	
mCol6α2	forward	TCCGAACCAAGCCCTTCGC	231
	reverse	CCCAAAGAGCCAGAGGACAC	
mCox4i1	forward	CCGTCTTGGTCTTCCGGTTG	111
	reverse	TGGAAGCCAACATTCTGCCA	
mCox5b	forward	GCTTCAAGGTTACTTCGCGG	184
	reverse	TGTATGGGTCCAGTCCCTTCT	
mCox8b	forward	GACCCCGAGAATCATGCCAA	131
	reverse	CCTGCTCCACGGCGGAA	
mCpt-1α	forward	TTGGAAGTCTCCCTCCTTCA	118
	reverse	GCCCATGTTGTACAGCTTCC	
mCpt-1β	forward	TCTCCATGGGACTGGTCGAT	239
	reverse	GAGACGGACACAGATAGCCC	
mDgat	forward	TAGAAGAGGACGAGGTGCGA	237

	reverse	TCAGGATCAGCATCACCACAC	
mDio2	forward	GAAGATGGGACTCCTCAGCG	238
	reverse	ACCCAGTTTAACCTGTTTGTAGG	
mFabp1	forward	CAATAGGTCTGCCCGAGGAC	193
	reverse	AGCTTGACGACTGCCTTGAC	
mFabp4	forward	AAACTGGGCGTGGAATTCGA	120
	reverse	TATTGTGGTCGACTTTCCAT	
mHsl	forward	GCCGGTGACGCTGAAAGTGGT	197
	reverse	CGCGCAGATGGGAGCAAGAGGT	
mIl-1β	forward	GACCTTCCAGGATGAGGACA	183
	reverse	AGCTCATATGGGTCCGACAG	
mIl-6	forward	GAGGATACCACTCCCAACAGACC	141
	reverse	AAGTGCATCATCGTTGTTCATACA	
miNOS	forward	AATCTTGGAGCGAGTTGTGG	139
	reverse	CAGGAAGTAGGTGAGGGCTTG	
mLeptin	forward	AAGGGGCTTGGGTTTTTCCA	133
	reverse	CAGACAGAGCTGAGCACGAA	
mMcp-1	forward	GCAGGTCCCTGTCATGCTTC	211
	reverse	CTTGAGCTTGGTGACAAAAACTAC	
mNdufb2	forward	GGAGTTTCCCCAGCTTACCC	217
	reverse	CTCACCTTGCTCTCGTCCAG	
mNF-κB p65	forward	CCTCTGGCGAATGGCTTTACT	163
	reverse	GTTGCTTCGGCTGTTCGAT	
mNogo-B	forward	TCGGGCTCAGTGGTTGTT	91
	reverse	GAGACAGCAGCAGGAATAAGCT	
mNrf1	forward	GCTGCAGGTCCTGTGGGAAT	148
	reverse	ACTCATCCAACGTGGCTCTG	
mPgc-1α	forward	CCCTGCCATTGTTAAGACC	161
	reverse	TGCTGCTGTTCCTGTTTTC	
mPrdm16	forward	CAGCACGGTGAAGCCATTC	87
	reverse	GCGTGCATCCGCTTGTG	
mScd-1	forward	CAGCCGAGCCTTGTAAGTTC	143
	reverse	GAGGCCTGTACGGGATCATA	
mTbx-1	forward	AGGCAGGCAGACGAATGTT	115
	reverse	TACCGGTAGCGCTTGTCATC	
mTnf-α	forward	CGTCGTAGCAAACCACCAAG	150
	reverse	TTGAAGAGAACCTGGGAGTAGACA	
mUcp-1	forward	ACTGCCACACCTCCAGTCATT	123
	reverse	CTTTGCCTCACTCAGGATTGG	
mVegf-β	forward	AGCCAGACAGGGTTGCCATA	272
	reverse	CTTGTCACTTTCGCGGCTTC	
mGapdh	forward	TGTGTCCGTCGTGGATCTGA	150
	reverse	TTGCTGTTGAAGTCGCAGGAG	

hIl-1β	forward	AGCCATGGCAGAAGTACCTG	116
	reverse	CCTGGAAGGAGCACTTCATCT	
hIl-6	forward	CCTTCGGTCCAGTTGCCTT	318
	reverse	TCACCAGGCAAGTCTCCTCAT	
hMcp-1	forward	TCCCAAAGAAGCTGTGATCTTCA	104
	reverse	TTTGCTTGTCCAGGTGGTCC	
hNF-κB p65	forward	CCTATAGAAGAGCAGCGTGGG	139
	reverse	TGGGGGCACGATTGTCAAAG	
hGapdh	forward	TGATGACATCAAGAAGGTGGTGAAG	240
	reverse	TCCTTGGAGGCCATGTGGGCCAT	

m, mus musculus; h, homo sapiens; Acaca, acetyl-CoA carboxylase α; Aco2, aconitase 2; Acox, acyl-CoA oxidase; AdipoR1, adiponectin receptor 1; Arg-1, arginase 1; Atf4, activating transcription factor 4; Atgl, adipose triglyceride lipase; Bip, heat shock protein family A member 5; Chop, C/EBP homologous protein; Cidea, cell death-inducing DNA fragmentation factor-alpha-like effector α; Col6α1, collagen type VI α1; Col6α2, collagen type VI α2; Cox4i1/5b/8b, cytochrome C oxidase subunit 4 isoform 1 or 5b or 8b; Cpt-1, carnitine palmitoyltransferase 1; Dgat, diacylglycerol *O*-acyltransferase; Dio2, deiodinase 2; Fabp1, fatty acid binding protein 1; Fabp4, fatty acid binding protein 4; Hsl, hormone-sensitive lipase; Il, interleukin; iNOS, inducible NO synthase; Mcp-1, monocyte chemoattractant protein 1; Ndufb2, NADH:ubiquinone oxidoreductase subunit b2; Nrf1, nuclear respiratory factor 1; Pgc-1α, peroxisome proliferator-activated receptor γ co-activator α; Prdm16, PR domain containing 16; Scd-1, stearoyl-CoA desaturase-1; Tbx-1, T-box transcription factor 1; Tnf-α, tumor necrosis factor α; Ucp-1, uncoupling protein-1; Vegf-β, vascular endothelial growth factor β; Gapdh, glyceraldehyde-3-phosphate dehydrogenase.

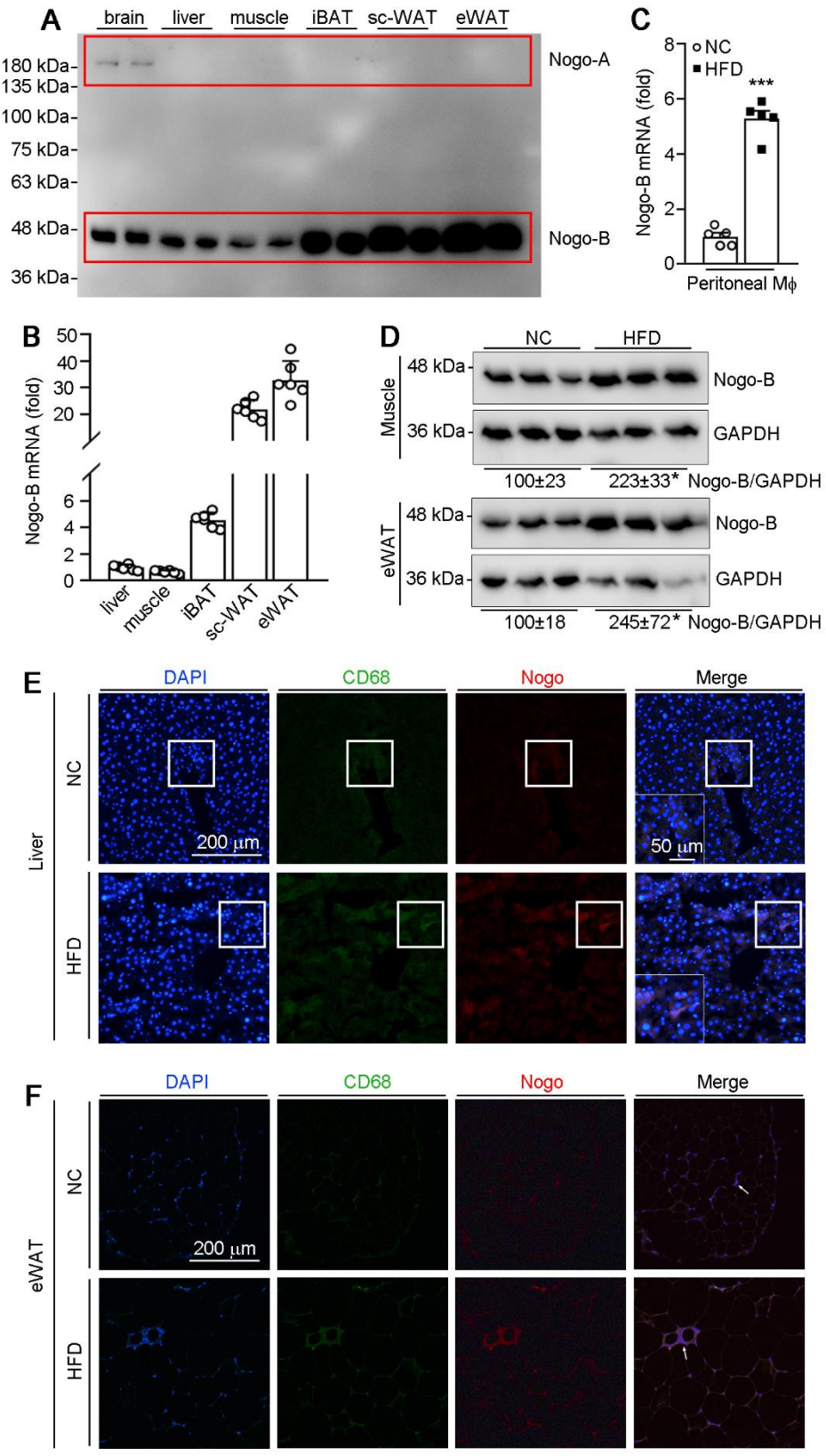

Figure S1. HFD upregulates Nogo expression in macrophages, muscle and eWAT

A, B: Brain, liver, skeletal muscle, iBAT, sc-WAT and eWAT samples collected from male control mice (~10-week old) were used to determine Nogo protein (**A**) and Nogo-B mRNA levels (**B**) by Western blot and qRT-PCR, respectively. **C**: C57BL/6J mice (males, ~6-week old) were fed normal chow (NC) or HFD for 10 weeks and peritoneal macrophages were collected to determine mRNA expression of Nogo-B by qRT-PCR (n=5). **D-F**: Liver, skeletal muscle and eWAT tissues collected from Figure 2 were conducted the following assays. Nogo-B protein expression in skeletal muscle and eWAT were determined by Western blot (**D**, n=3). Liver (**E**) and eWAT (**F**) sections were conducted co-immunofluorescent staining with CD68 (marker for macrophages) and Nogo antibodies. *$p < 0.05$, ***$p < 0.001$ *versus* control NC-fed mice. eWAT, epididymal white adipose tissue; HFD, high-fat diet; iBAT, interscapular brown adipose tissue; NC, normal chow; Nogo, reticulon-4; qRT, quantitative RT; sc-WAT, subcutaneous white adipose tissue.

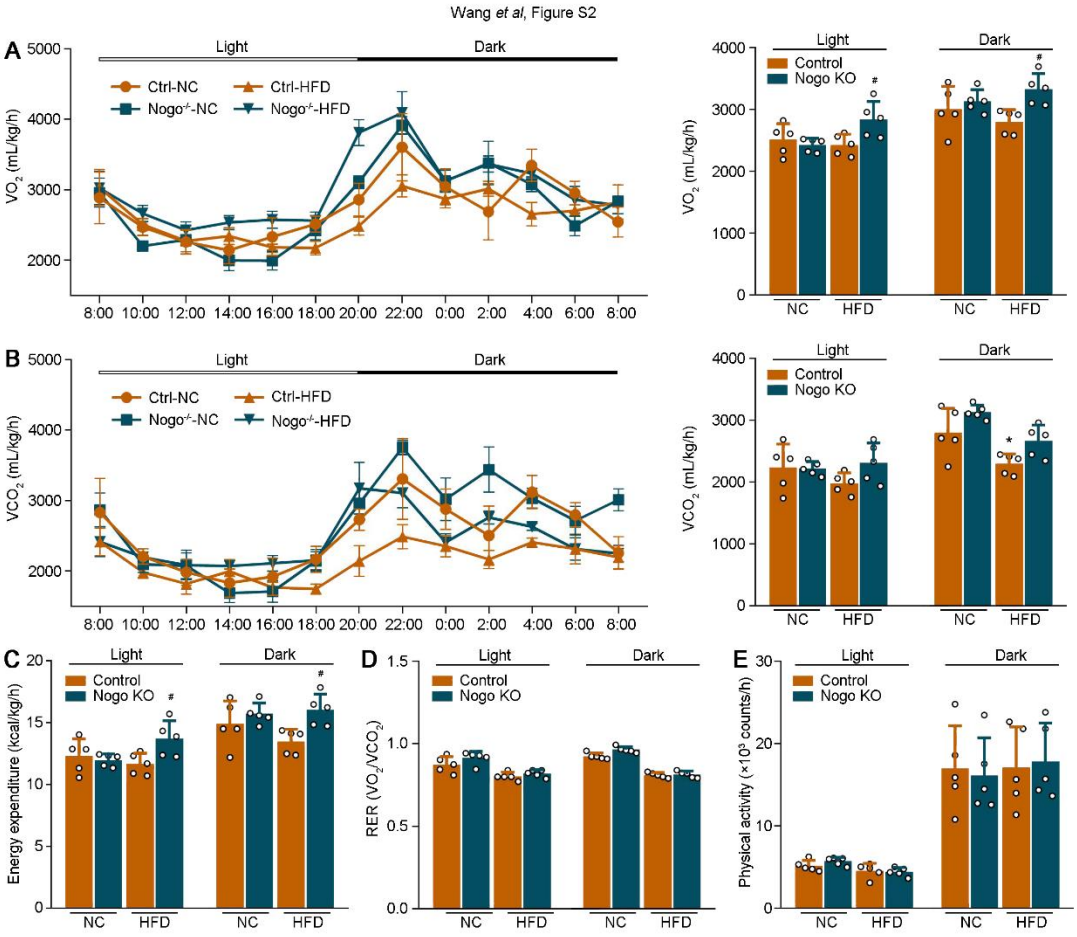

Figure S2. Nogo deficiency increases oxygen consumption and energy expenditure

Male control and Nogo$^{-/-}$ mice (~6-week old) were fed normal chow (NC) or HFD for 10 weeks. Oxygen consumption (**A**) and carbon dioxide production (**B**) were determined by indirect calorimetry. Energy expenditure (**C**) and respiratory exchange rate (RER, **D**) was calculated. Locomotor activity was determined by counting infrared light beam breaks (**E**) (n=5). *$p < 0.05$ *versus* control NC-fed mice; $^{\#}p < 0.05$ *versus* control HFD-fed mice. HFD, high-fat diet; NC, normal chow; Nogo, reticulon-4.

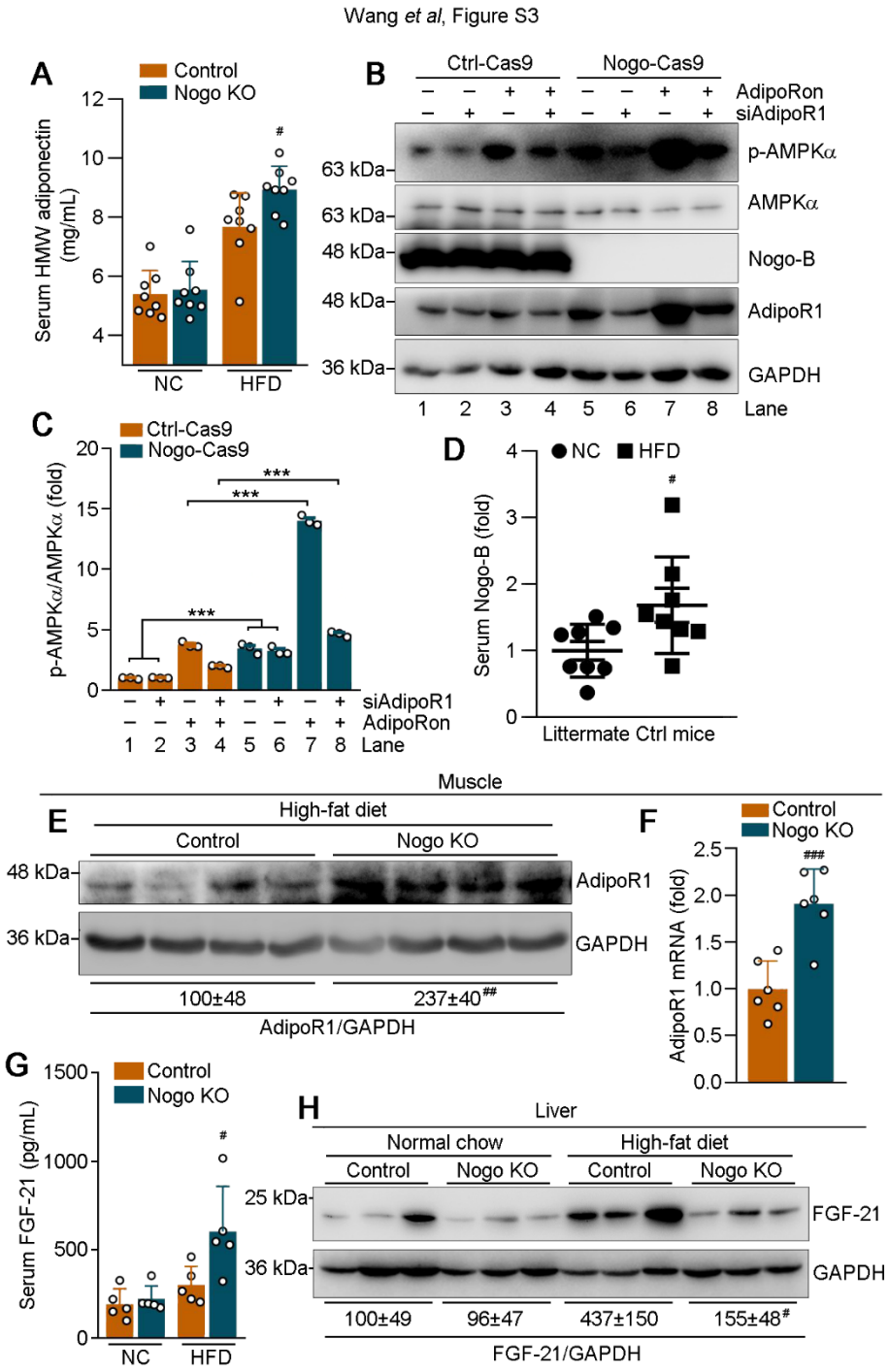

Figure S3. Regulation of HMW adiponectin, AMPKα, AdipoR1 and FGF-21 by Nogo

A, D-H: Mouse serum, skeletal muscle and liver samples collected from Figure 2 were used to determine HMW adiponectin (**A**, n=8), Nogo-B (**D**, littermate control mice only, n=8) and FGF-21 (**G**, n=5) levels in serum with the corresponding Elisa kits. Expression of AdipoR1 in skeletal muscle (n=4, **E**) and FGF-21 in liver (n=3, **H**) was determined by Western blot with quantitative analysis of band density. Expression of AdipoR1 mRNA in skeletal muscle (**F**) was determined by qRT-PCR (n=6). $^{\#}P<0.05$, $^{\#\#}p < 0.01$, $^{\#\#\#}p < 0.001$ *versus* control HFD-fed mice.

B, C: Ctrl-Cas9 or Nogo-Cas9 HepG2 cells were transfected with control siRNA or AdipoR1

siRNA for 24 h, then treated with AdipoRon (10 μmol/l) for 16 h. Protein expression of Nogo-B, AdipoR1, p-AMPKα and AMPKα were determined by Western blot (**B**) with quantitative analysis of the ratio of band density of p-AMPKα to AMPKα (**C**, n=3). ***$p < 0.001$. AdipoR1, adiponectin receptor 1; AMPKα, AMP-activated kinase α; FGF-21, fibroblast growth factor 21; HMW, high-molecular weight; NC, normal chow; Nogo, reticulon-4; p-AMPKα, phosphorylated AMP-activated kinase α; qRT, quantitative RT.

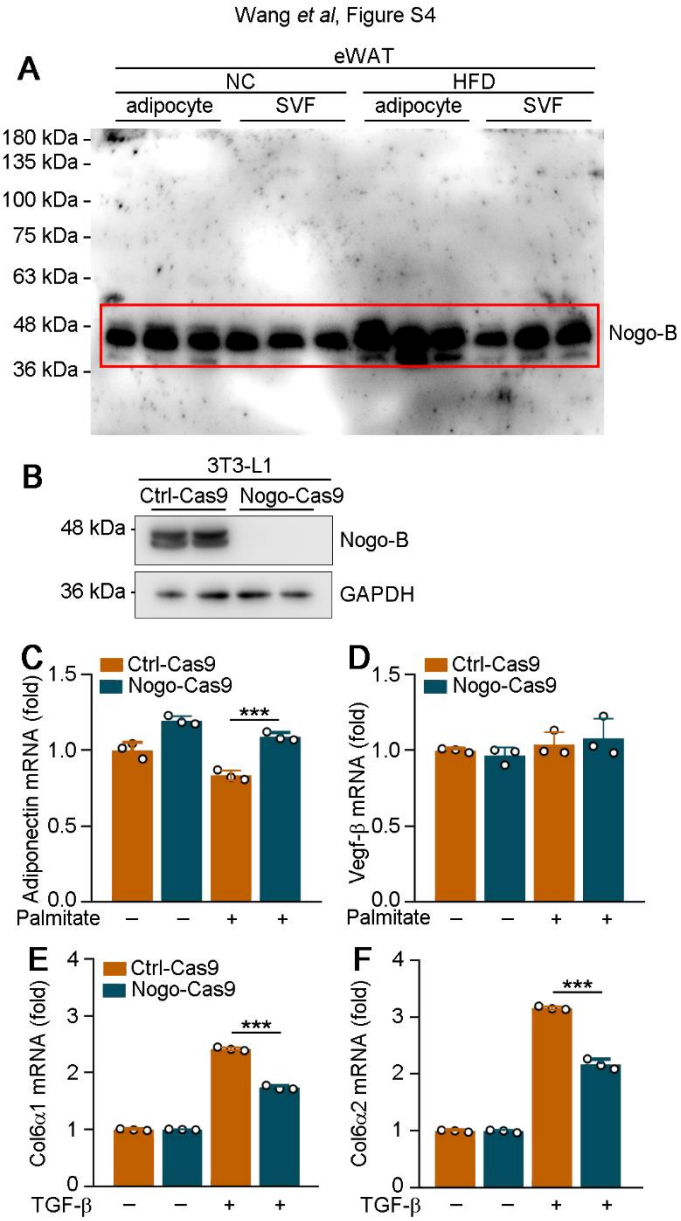

Figure S4. Nogo deficiency regulates expression of adiponectin and collagen VI partly in a cell-autonomous manner

A: male control mice (~6-week old) were fed normal chow (NC) or HFD for 10 weeks. Adipocytes and stromal vascular fractions (SVF) were collected from eWAT to determine Nogo protein expression by Western blot (n=3). **B-F**: Control (Ctrl-Cas9) and Nogo deficient (Nogo-Cas9) 3T3-L1 preadipocytes were constructed using CRISPR/Cas9 technology. Nogo protein expression was determined by Western blot (**B**). Ctrl-Cas9 and Nogo-Cas9 3T3-L1 preadipocytes were induced to mature adipocytes, followed by treatment with 200 μmol/l palmitate for 16 h (**C, D**) or 15 ng/ml TGF-β for 48 h (**E, F**). mRNA expression of Adiponectin (**C**), Vegf-β (**D**), Col6α1 (**E**) and Col6α2 (**F**) was determined by qRT-PCR (n=3). ***$p < 0.001$. Col6α1/α2, collagen type VI α1 or α2; eWAT, epididymal white adipose tissue; HFD, high-fat diet; NC, normal chow; Nogo, reticulon-4; qRT, quantitative RT; TGF-β, transforming growth factor β; Vegf-β, vascular endothelial growth factor β.

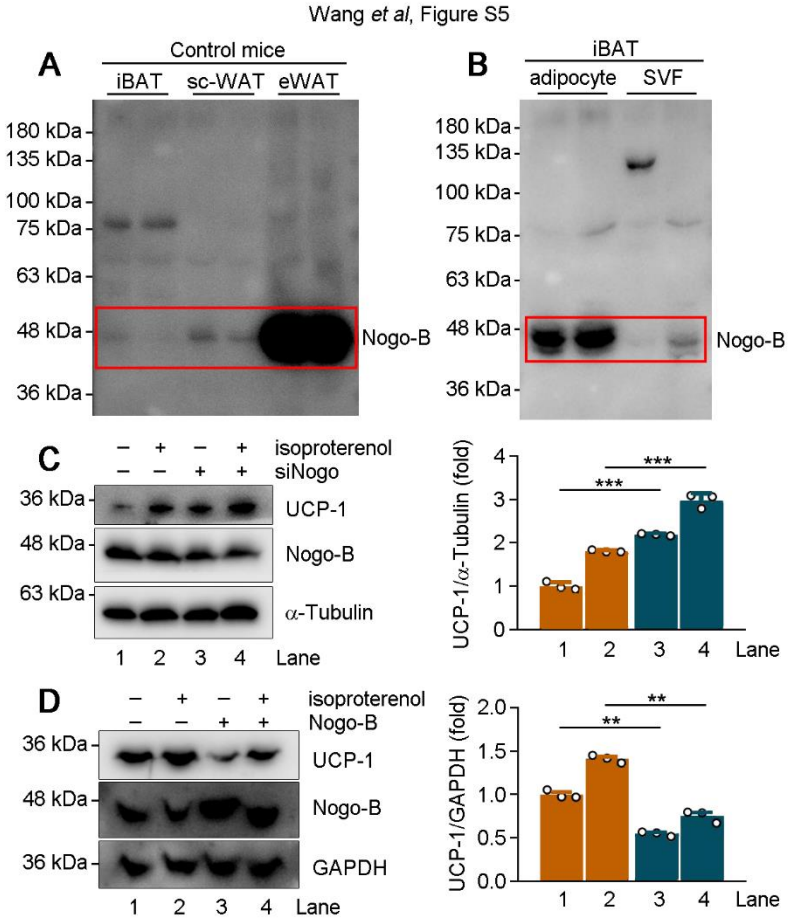

Figure S5. Nogo regulates thermogenesis partly in a cell-autonomous manner

A: iBAT, sc-WAT and eWAT samples collected from control mice in Figure 4G were used to determine Nogo protein expression by Western blot. **B**: adipocytes and stromal vascular fractions (SVF) collected from male control mice (~10-week old) iBAT were used to determine Nogo protein expression by Western blot. **C, D**: Mature adipocytes derived from C3H10T1/2 cells were transfected with Nogo siRNA (**C**) or mouse Nogo-B expression vector (**D**) for 24 h, then treated with 10 μmol/l isoproterenol for 16 h. Protein expression of UCP-1 and Nogo-B was determined by Western blot with quantitative analysis (n=3). $^{**}p < 0.01$; $^{***}p < 0.001$. iBAT, interscapular brown adipose tissue; Nogo, reticulon-4; UCP-1, uncoupling protein 1.

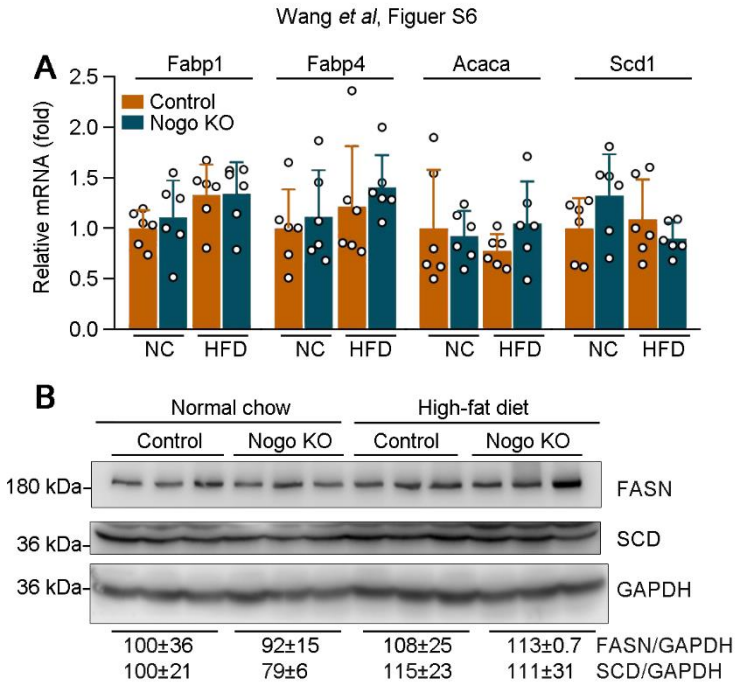

Figure S6. Nogo deficiency has little effect on expression of fatty acid uptake- or synthesis-related genes in the liver

Liver samples collected from mice in Figure 2 were conducted the following assays. **A**: expression of fatty acid uptake (Fabp1 and Fabp4)- and synthesis (Acaca and Scd1)-related genes were determined by qRT-PCR (n=6). **B**: protein expression of FASN and SCD was determined by Western blot with quantitative analysis of band density (n=3). Acaca, acetyl-CoA carboxylase α; Fabp1/4, fatty acid binding protein 1 or 4; FASN, fatty acid synthase; HFD, high-fat diet; NC, normal chow; Nogo, reticulon-4; qRT, quantitative RT; SCD, stearoyl-CoA desaturase.

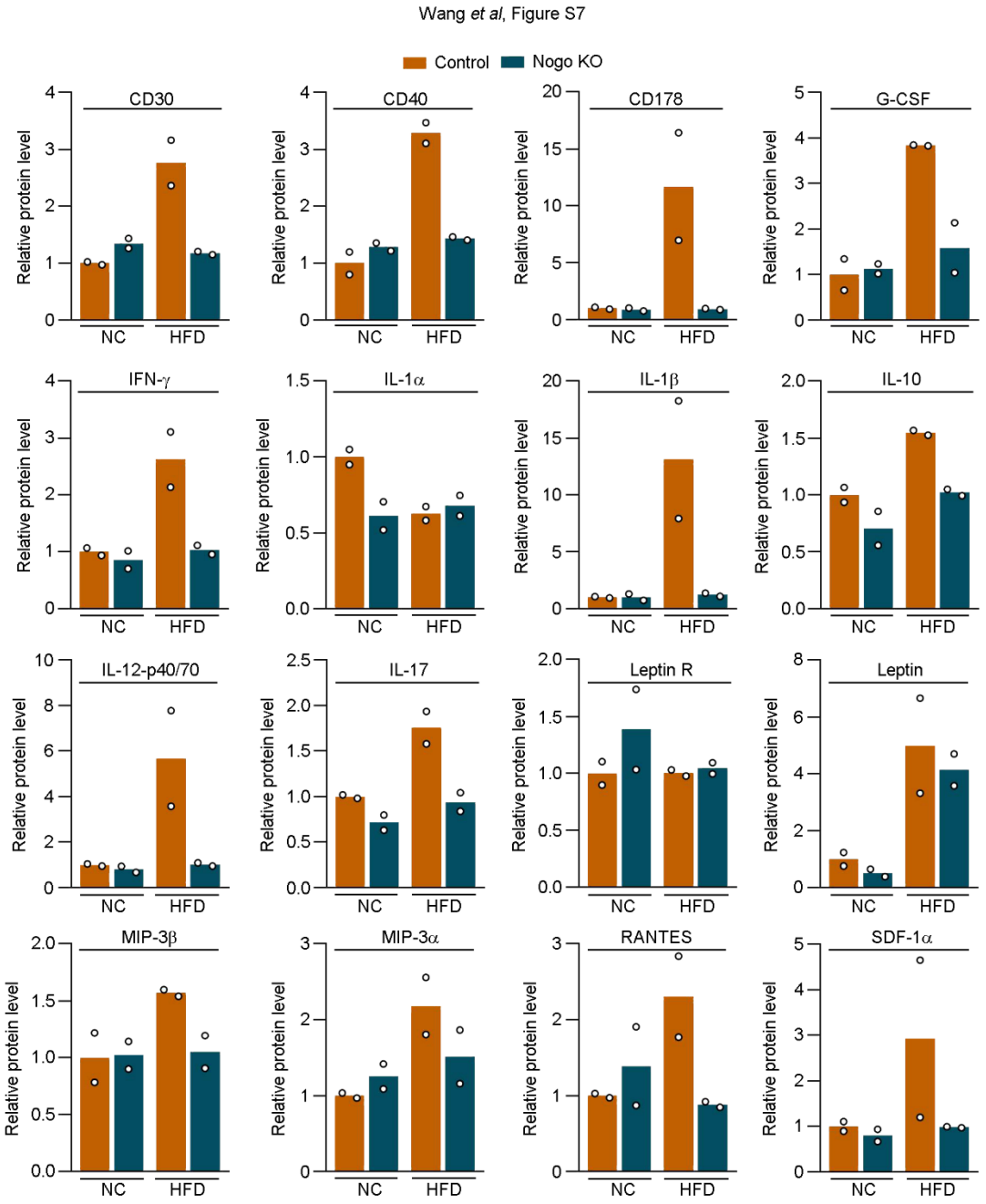

Figure S7. Nogo deficiency reduces serum inflammatory cytokines in HFD-fed mice

Mouse serum samples collected from Figure 2 were used to determine expression of inflammatory cytokines by the mouse cytokine array G3 method (RayBiotech) as shown in Figure 6**A** (n=2). Levels of inflammatory cytokines were also semi-quantitatively analyzed and presented in this figure. CD30, tumor necrosis factor receptor superfamily, member 8; CD40, tumor necrosis factor receptor superfamily, member 5; CD178, FAS ligand; G-CSF, granulocyte colony stimulating factor; HFD, high-fat diet; IFN-γ, interferon γ; IL-1α/1β/10/17, interleukin 1α or 1β or 10 or 17; IL-12-p40/p70, interleukin 12 subunit β/subunit α; Leptin R, leptin receptor; MIP-3β/3α, C-C motif chemokine ligand 19 or 20; NC, normal chow; Nogo, reticulon-4; RANTES, C-C motif chemokine ligand 5; SDF-1α, C-X-C motif chemokine ligand 12.

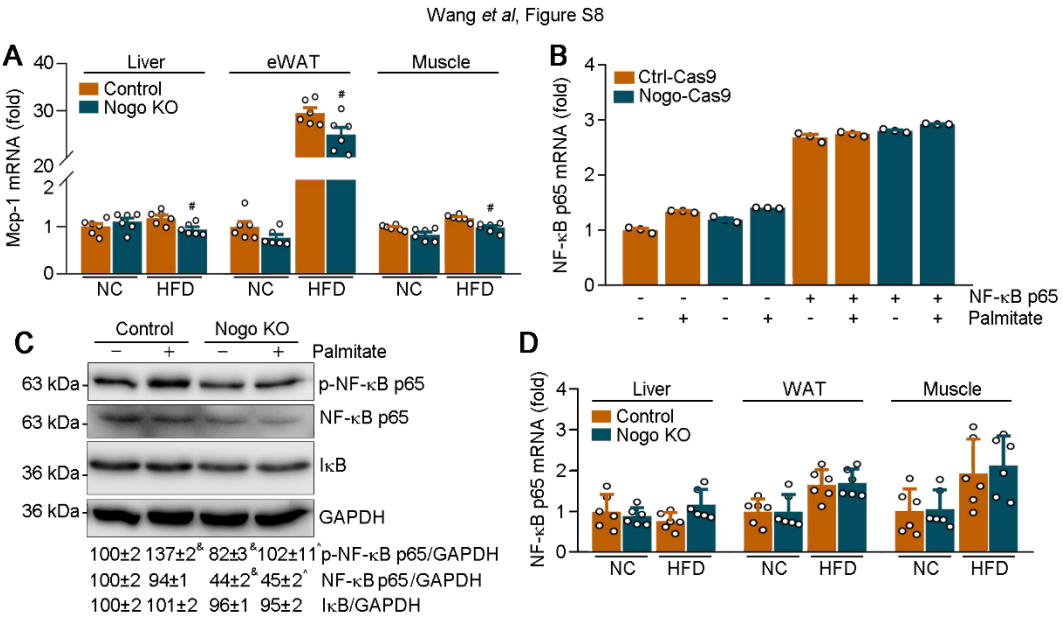

Figure S8. Nogo regulates Mcp-1 mRNA expression independent on IκB expression

A, D: Liver, skeletal muscle and eWAT samples collected from Figure 2 were used to determine Mcp-1 (**A**) and NF-κB p65 (**D**) mRNA expression by qRT-PCR (n=6). $^{\#}p < 0.05$ *versus* control HFD-fed mice. **B**: Ctrl-Cas9 or Nogo-Cas9 HepG2 cells were transfected with NF-κB p65 expression vector for 24 h, followed by 200 μmol/l palmitate treatment for 16 h. mRNA expression of NF-κB p65 was determined by qRT-PCR. **C**: Peritoneal macrophages collected from control or Nogo$^{-/-}$ mice were treated with 200 μmol/l palmitate for 16 h. Protein expression of p-NF-κB p65 (the active form of NF-κB in nucleus), NF-κB p65 and IκB was determined by Western blot with quantitative analysis (n=3). $^{\&}p < 0.05$ *versus* control cells; $^{\wedge}p < 0.05$ *versus* palmitate treated control cells. eWAT, epididymal white adipose tissue; HFD, high-fat diet; Mcp-1, monocyte chemoattractant 1; NC, normal chow; Nogo, reticulon-4; qRT, quantitative RT.

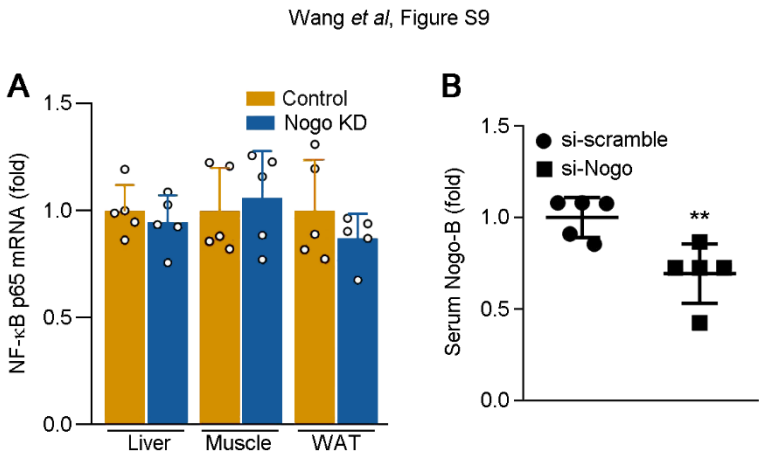

Figure S9. si-Nogo decreases serum Nogo-B levels while has little effect on NF-κB p65 mRNA expression in mouse tissues

Mouse serum, liver, skeletal muscle and WAT samples collected from Figure 9 were used to determine NF-κB p65 mRNA expression in tissues (**A**) and Nogo-B levels in seurm (**B**) using qRT-PCR and Elisa kits, respectively. $^{**}p < 0.01$ *versus* control mice, n=5. Nogo, reticulon-4; qRT, quantitative RT; WAT, white adipose tissue.

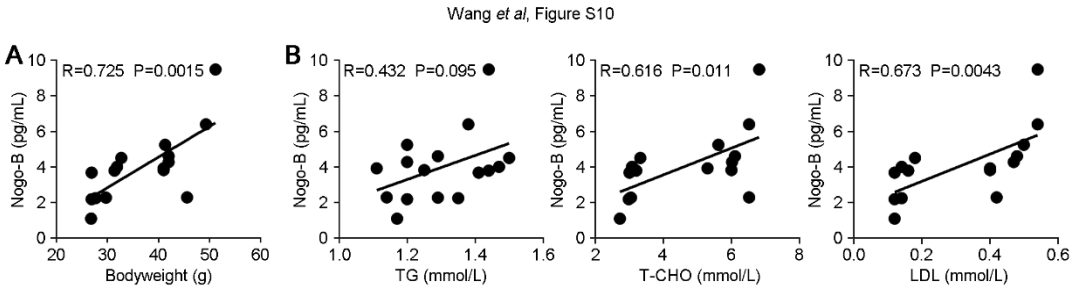

Figure S10. Serum Nogo-B is correlated with mouse bodyweight, serum T-CHO and LDL levels

Mice serum samples collected from Figure 2 were used to determine levels of Nogo-B, TG, T-CHO and LDL. The correlation coefficient between Nogo-B and mice bodyweight (**A**) or lipid profiles (**B**) was analyzed using the Pearson correlation test with 95% confidence interval. LDL, low-density lipoprotein cholesterol; Nogo, reticulon-4; T-CHO, total cholesterol; TG, triglyceride.

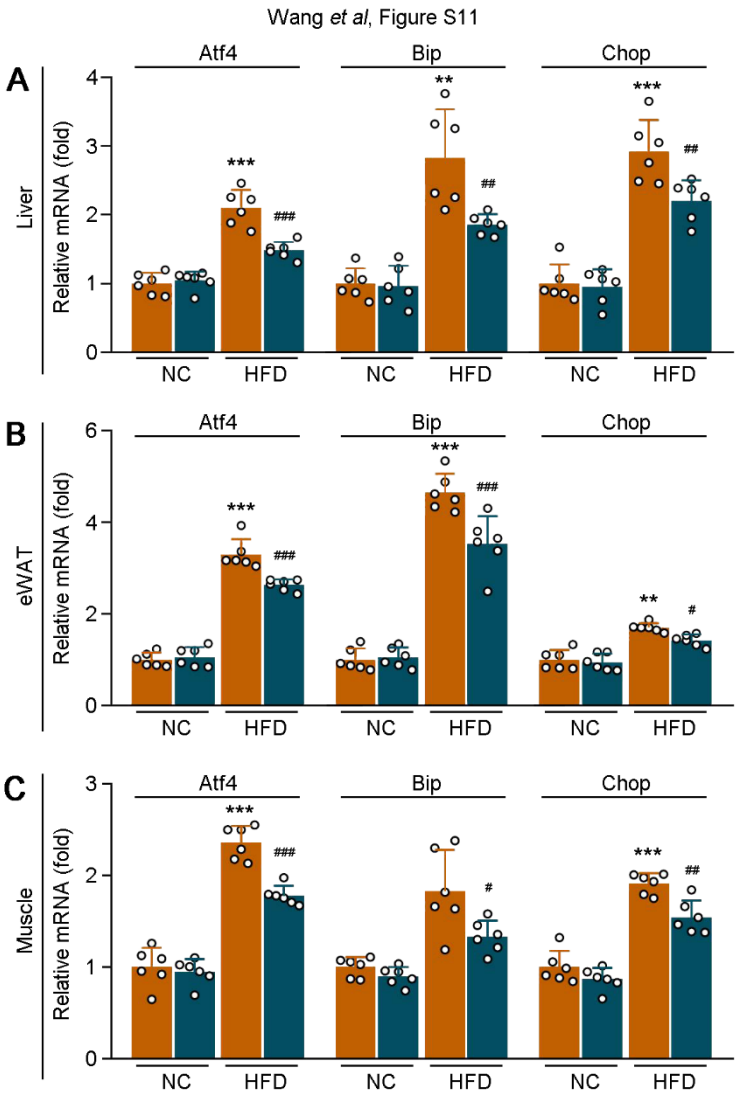

Figure S11. Nogo deficiency decreases obesity-induced expression of ER stress-related genes in liver, eWAT and skeletal muscle

Liver (**A**), eWAT (**B**) and skeletal muscle (**C**) samples collected from mice in Figure 2 were used to determined mRNA expression of Atf4, Bip and Chop by qRT-PCR (n=6). $^{**}p < 0.01$, $^{***}p < 0.001$ *versus* control NC-fed mice; $^{\#}p < 0.05$, $^{\#\#}p < 0.01$, $^{\#\#\#}p < 0.001$ *versus* control HFD-fed mice. Atf4, activating transcription factor 4; Bip, heat shock protein family A member 5; Chop, C/EBP homologous protein; eWAT, epididymal white adipose tissue; HFD, high-fat diet; NC, normal chow; Nogo, reticulon-4; qRT, quantitative RT.

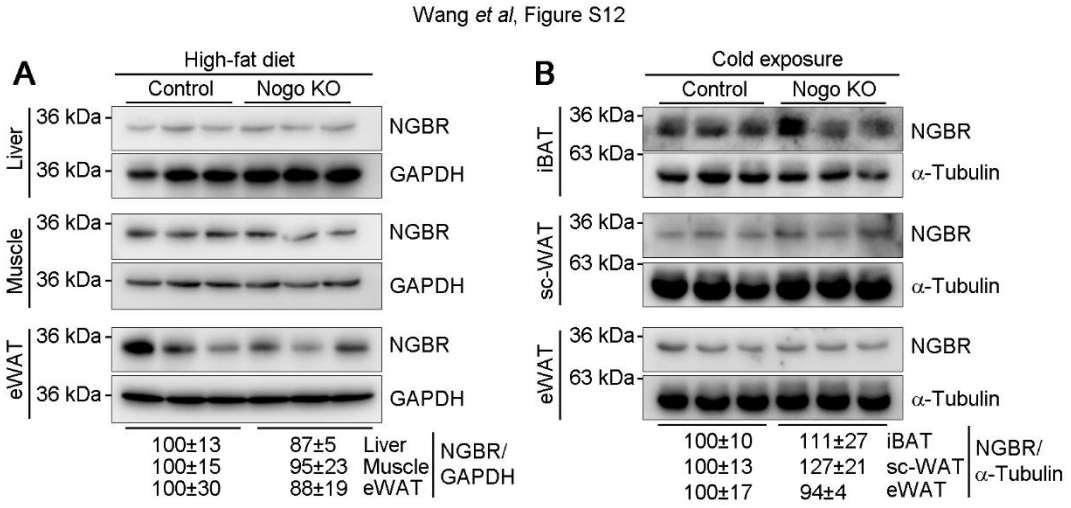

Figure S12. Nogo deficiency has little effect on NGBR protein expression under different conditions

Liver, skeletal muscle and eWAT samples collected from mice in Figure 2 (**A**), and iBAT, sc-WAT and eWAT samples collected from Figure 4G (**B**) were used to determined NGBR protein expression by Western blot with quantitative analysis (n=3). eWAT, epididymal white adipose tissue; iBAT, interscapular brown adipose tissue; NGBR, Nogo-B receptor; Nogo, reticulon-4; sc-WAT, subcutaneous white adipose tissue.

Supplemental experimental procedures

Materials

Isoproterenol (catalog no.: HY-B0468), transforming growth factor β (catalog no.: HY-P7119), indomethacin (catalog no.: HY-14397), 3,3,5-triiodo-L-thyronine (catalog no.: HY-A0070A), dexamethasone (catalog no.: HY-14648) and isobutylmethylxanthine (catalog no.: HY-12318) were purchased from Medchemexpress. Insulin (catalog no.: I2643) was purchased from Sigma-Aldrich.

Determination of oxygen consumption and physical activity

After 10-week normal chow or HFD feeding, mice were housed individually in indirect calorimeter chambers (TSE System) in a 12-h light/12-h dark cycle with free access to food and water. All mice were acclimatized for 24 h prior to measurements. Oxygen consumption (VO_2), carbon dioxide production (VCO_2) and respiratory exchange rate (RER) were measured over the course of the next 24 h. Physical activity was determined by counting infrared light beam breaks. Energy expenditure was calculated using the following equation: $(3.815+1.232\times RER) \times VO_2$.

Cell culture

3T3-L1 fibroblast was purchased from American Type Culture Collection and cultured in Dulbecco's modified Eagle's medium containing 10% bovine calf serum, 50 μg/ml penicillin/streptomycin with 2 mmol/l glutamine. C3H10T1/2 cell line was generously provided by Professor Changqing Zuo and cultured in minimum essential medium containing 10% fetal bovine serum, 50 μg/ml penicillin/streptomycin.

3T3-L1 cells lacking Nogo-B expression were established using CRISPR/Cas9 technology as described (1), and named as Nogo-Cas9 cells, while the corresponding control cells were named as Ctrl-Cas9 cells.

White adipocyte differentiation was induced as described (2). Briefly, 3T3-L1 cells were differentiated in Dulbecco's modified Eagle's medium containing 10% bovine calf serum, 1 μmol/l dexamethasone, 10 μg/ml insulin and 0.5 mmol/l isobutylmethylxanthine. After 3 days, cells were switched to the maintenance medium (Dulbecco's modified Eagle's medium containing 10% bovine calf serum and 10 μg/ml insulin) for another 10 days. For transforming growth factor β treatment, 15 ng/ml transforming growth factor β was added into maintenance medium in the last 2 days of induction. For palmitate treatment, 200 μmol/l palmitate was added into Dulbecco's modified Eagle's medium after cell induction.

Brown adipocyte differentiation was induced as described (3). Briefly, C3H10T1/2 cells were cultured in minimum essential medium containing 10% fetal bovine serum, 5 μg/ml insulin, 1 μmol/l dexamethasone, 0.5 mmol/l isobutylmethylxanthine, 120 μmol/l indomethacin and 1 nmol/l 3,3,5-triiodo-L-thyronine, then in MEM medium containing 10% fetal bovine serum, 5 μg/ml insulin and 1 nmol/l 3,3,5-triiodo-L-thyronine for another 6 days. For Nogo knockdown experiment, C3H10T1/2 cells derived adipocytes were transfected with Nogo siRNA using Lipofectamine RNAiMAX Reagent for 24 h. For Nogo overexpression experiment, Nogo expression vector was transfected into C3H10T1/2 cells derived adipocytes by Bio-Rad Gene Pulser Xcell^{TM} Electroporator for 24 h. Then, cells were treated with 10 μmol/l isoproterenol for 16 h.

To collect peritoneal macrophages, mice were euthanized, followed by collection of peritoneal macrophages using the method of PBS peritoneal lavage as described (4). The suspension of peritoneal macrophages in PBS was centrifuged for 3 min at 800*g*. Cell pellet was re-suspended in the red-blood-cell lysis buffer and incubated for 1 min. After addition of PBS, the suspension was centrifuged for another 3 min at 800*g*. Cell pellet was re-suspended in Roswell Park Memorial Institute 1640 medium containing 10% fetal bovine serum, 50 μg/ml penicillin and streptomycin, and 2 mmol/l glutamine, and cultured for two days before the indicated treatment in serum-free medium.

Collection of adipocytes and stromal vascular fraction (SVF) from white or brown adipose tissue

Adipocytes and SVFs were collected as described with minor modification (5). Fresh epididymal white adipose tissue or interscapular brown adipose tissue was minced into small pieces, then digested in a dissociation buffer (10 mg/ml BSA, 2 mmol/l glucose, 4 mg/ml collagenase type II in PBS) under slow continuous rotation (200 rpm) for 30 min at 37 °C. After digestion, the mixture was filtered through a 100 μm filter. After 1 min, floating adipocytes were transferred into a new tube. SVFs in the remaining solution were collected by centrifugation at 500 *g* for 8 min.

Determination of Nogo protein expression in mouse tissues

Total cellular protein was extracted from mouse tissues (brain, liver, muscle, interscapular brown adipose, subcutaneous white adipose tissue, epididymal white adipose). The same amount of protein (40 μg) from each sample was used to determine protein expression of Nogo family members by Western blot.

Plasmid construction

Mouse Nogo-B expression vector was generated using complementary DNA from 3T3-L1 cells, followed by PCR with forward and reverse primers of 5'-CAGaagcttATGGAAGACATAGACCAGTC-3' and 5'-CAGgaattcTCATTCTGCTTTGCGCTTCA-3'. Letters in lowercase represent the restriction sites of HindIII and EcoRI, respectively. The PCR product was digested with HindIII and EcoRI, and then ligated into a pcDNA3.1(+) plasmid.

Reference

1. Zhang, S., Yu, M., Guo, F., Yang, X., Chen, Y., Ma, C., Li, Q., Wei, Z., Li, X., Wang, H., Hu, H., Zhang, Y., Kong, D., Miao, Q. R., Hu, W., Hajjar, D. P., Zhu, Y., Han, J., and Duan, Y. (2020) Rosiglitazone alleviates intrahepatic cholestasis induced by alpha-naphthylisothiocyanate in mice: The role of circulating 15-deoxy-Delta(12,14) -PGJ_2 and Nogo. *Br J Pharmacol* **177**, 1041-1060
2. Rotter, D., Peiris, H., Grinsfelder, D. B., Martin, A. M., Burchfield, J., Parra, V., Hull, C., Morales, C. R., Jessup, C. F., Matusica, D., Parks, B. W., Lusis, A. J., Nguyen, N. U. N., Oh, M., Iyoke, I., Jakkampudi, T., McMillan, D. R., Sadek, H. A., Watt, M. J., Gupta, R. K., Pritchard, M. A., Keating, D. J., and Rothermel, B. A. (2018) Regulator of Calcineurin 1 helps coordinate whole-body metabolism and thermogenesis. *EMBO Rep* **19**, 44706
3. Zhang, Y., Li, J., Wang, H. H., Li, J., Yu, Y., Li, B., Huang, L., Wu, C., and Liu, X. (2021) Phytohemagglutinin ameliorates HFD-induced obesity by increasing energy expenditure. *J Mol Endocrinol* **67**, 1-14
4. Yang, X., Zhang, W., Chen, Y., Li, Y., Sun, L., Liu, Y., Liu, M., Yu, M., Li, X., Han, J., and Duan, Y. J. (2016) Activation of peroxisome proliferator-activated receptor γ (PPAR γ) and CD36 protein expression: The dual pathophysiological roles of progesterone. *J Biol Chem* **291**, 15108-15118
5. Methlie, P., Dankel, S., Myhra, T., Christensen, B., Gjerde, J., Fadnes, D., Vage, V., Lovas, K., and Mellgren, G. (2013) Changes in adipose glucocorticoid metabolism before and after bariatric surgery assessed by direct hormone measurements. *Obesity (Silver Spring)* **21**, 2495-2503